Invited Review

Chinese Science Bulletin

Biophysics

December 2013 Vol.58 No.36: 4519–4527
doi: 10.1007/s11434-013-6088-4

Super-resolution microscopy of live cells using single molecule localization

ZHANG YongDeng[1†], CHANG Hao[2†], GU LuSheng[1], ZHAO YanHua[3], XU Tao[1,3*] & JI Wei[3*]

[1] *School of Life Science and Technology, Huazhong University of Science and Technology, Wuhan 430074, China;*
[2] *School of Life Science, University of Science and Technology of China, Hefei 230027, China;*
[3] *Institute of Biophysics, Chinese Academy of Sciences, Beijing 100101, China*

Received January 29, 2013; accepted April 11, 2013

The resolution of conventional light microscopy is insufficient for subcelluar studies. The invention of various super-resolution imaging techniques breaks the diffraction barrier and pushes the resolution limit towards the nanometer scale. Here, we focus on a category of super-resolution microscopy that relies on the stochastic activation and precise localization of single molecules. A diversity of fluorescent probes with different characteristics has been developed to achieve super-resolution imaging. In addition, with the implementation of robust localization algorithms, this family of approaches has been expanded to multi-color, three-dimensional and live cell imaging, which provides a promising prospect in biological research.

resolution, super-resolution microscopy, single molecules, fluorescent probes, localization algorithms

Citation: Zhang Y D, Chang H, Gu L S, et al. Super-resolution microscopy of live cells using single molecule localization. Chin Sci Bull, 2013, 58: 4519–4527, doi: 10.1007/s11434-013-6088-4

Fluorescence microscopy has become an indispensable tool for cell biology. Because of the issue of diffraction, the resolution of traditional light microscopy is restricted to approximately 200 nm in lateral and 500 nm in axial direction. However, the last decade has witnessed the emergence and development of various super-resolution imaging techniques that break the diffraction barrier and shed light on cell biological questions that remain unanswered at subcellular level. Generally, these super-resolution microscopy approaches can be divided into two primary categories. The first strategy uses a nonlinear optical process or patterned illumination to spatially modulate the behavior of fluorescence, including stimulated emission depletion (STED) microscopy [1] and the related reversible saturable optically linear fluorescent transitions (RESOLFT) technology [2], as well as structured illumination microscopy (SIM) [3] and saturated structured illumination microscopy (SSIM) [4]. The second strategy stochastically activates, images and localizes individual molecules, from which super-resolution images can be reconstructed. This approach has been named photoactivated localization microscopy (PALM) [5], fluorescence PALM (FPALM) [6], stochastic optical reconstruction microscopy (STORM) [7] and direct STORM (dSTORM) [8]. Both categories have achieved sub-diffraction-limit imaging and improved the resolution by an order of magnitude. Here, we review the evolution of single molecule localization microscopy (SMLM), from its conception to its current state, and from the advent of fluorescent probes to the development of localization algorithms.

1 Concept of single molecule localization microscopy

In optical microscopy, when a single point source is focused through an objective lens, a diffraction-limited blurred spot appeared as the Airy disk point spread function (PSF) (Figure 1(a)). The resolution limit of point sources is quantified by the Rayleigh criterion which is defined in terms of the

†These authors contributed equally to this work.
*Corresponding authors (email: jiwei2188@gmail.com; xutao@ibp.ac.cn)

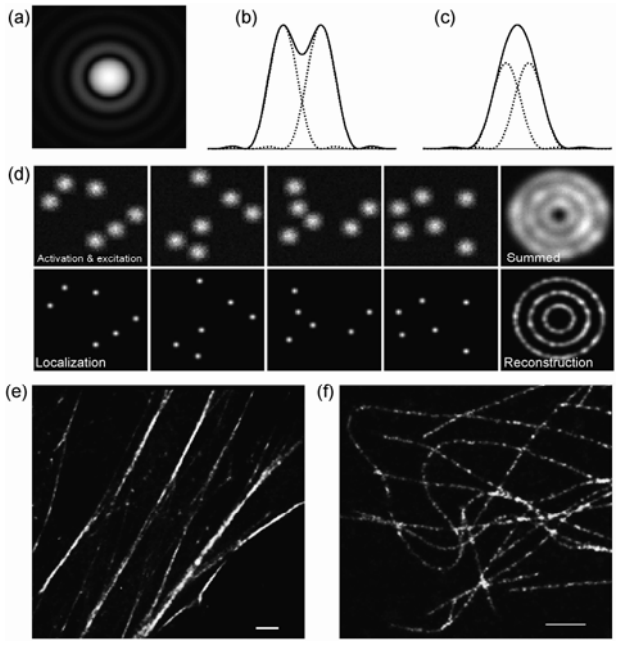

Figure 1 The concept of single molecule localization microscopy. (a) The Airy disk point spread function of optical microscopy. The image is displayed using a nonlinear intensity scale. (b) The Rayleigh criterion is defined in terms of the distance at which the principal maximum of one Airy disk coincides with the first minimum of the second Airy disk. (c) Two emitters cannot be resolved, when the distance is smaller than the Rayleigh criterion. (d) The imaging and analysis process of single molecule localization microscopy. (e) PALM image of HeLa cells expressing actin labeled with LifeAct-mEos3.2. (f) STORM image of COS-7 cells expressing β-tubulin labeled with Alexa Fluor 647. Scale bars are 2 μm in (e) and 1 μm in (f).

distance at which the principal maximum of one Airy disk coincides with the first minimum of the second Airy disk (Figure 1(b)). For monochromatic images of a given fluorescence wavelength, the Rayleigh criterion can be estimated as $r = 0.61\lambda/NA$, where λ is the wavelength of emission light and NA is the numerical aperture of the objective. Consequently, two light emitters separated by a distance less than r cannot be resolved and will appear as one subject (Figure 1(c)). Nevertheless, it has been proved that a single molecule can be localized with a precision well beyond the diffraction limit, which in theory, can be exploited for super-resolution imaging [9]. The problem lies in the fact that the fluorophores in labeled samples are densely distributed and many of them locates in the same diffraction-limited region. The emission from these fluorophores will overlap, making it impossible to achieve single molecule localization. Therefore, the key is to produce and localize spare subsets of molecules, which lead to the development of SMLM such as (F)PALM/(d)STORM. Generally, in this family of methods, one laser of a specific wavelength is used for the activation and the other for the excitation of fluorophores. The trick is to control the power and exposure time so that only a few fluorophores are imaged at each frame. After that, the position of these single molecules can be obtained by fitting the images with two-dimensional (2D) Gaussian function or other localization algorithms [10]. This process can be repeated many times until the accumulation of single molecules reaches a certain density to fulfill the Nyquist spatial sampling requirement (Figure 1(d)). Finally, super-resolution images can be reconstructed from these sparely distributed single molecules by assigning each localization to one point (e.g. a cross or a normalized 2D Gaussian peak) (Figure 1(e), (f)).

2 Fluorescent probes

The basic principle of SMLM using fluorescent probes is that their fluorescent spectrum can be altered through light-dependent [5−7] or light-independent methods [11,12]. An ideal probe to be used for this new technique should have three properties: (i) a one-to-one relationship with each protein to be studied, which avoids mislabeling and is important for quantitative analysis; (ii) high level of brightness and low background signals at the single molecule level, which improves the localization precision; (iii) high labeling density, which improves the Nyquist resolution. Although many fluorescent proteins, synthetic dyes and quantum dots have emerged as probes for SMLM, none of them possess all of these characteristics.

Compared to synthetic dyes and quantum dots, fluorescent proteins can be genetically encoded together with a protein of interest at a one-to-one ratio without encountering the problem of mislabeling (Table S1). This is a major advantage of this class of FPs, which is widely used in single-particle tracking PALM (sptPALM) [13] and single molecule counting [14]. In comparison, the major advantages of choosing synthetic dyes and quantum dots are their excellent photon budget, good contrast and outstanding photostability, which give higher localization precision and better reconstruction images [15,16]. Nowadays, labeling density of fluorescent probes has become an important factor to evaluate quality of SMLM images [17]. The Nyquist criterion, which is independent of localization precision, also should be considered in live cell SMLM imaging [18]. In general, the 2D Nyquist resolution resulting from the label density can be calculated as

$$\alpha_{\text{Nyquist}} = \frac{1}{a^{1/d}}, \tag{1}$$

where a is the label density and d is the dimension (in this case $d = 2$) [18]. Then the final resolution of images can be calculated as

$$\alpha^2_{\text{final}} = \alpha^2_{\text{localization}} + \alpha^2_{\text{Nyquist}}, \tag{2}$$

where α^2_{final} is the effective spatial resolution, $\alpha^2_{\text{localization}}$ is the localization precision and $\alpha^2_{\text{Nyquist}}$ is the Nyquist resolution [19].

2.1 Fluorescent proteins

Although some conventional fluorescent proteins (FPs), such as EGFP and mCherry, have been used in some super-resolution techniques like SIM and STED, only certain FPs, which alter their photophysical properties at specific light illumination, could be used in SMLM imaging. Over 30 different members of the FP family have been discovered or developed, and with few exceptions, they can be classified into the following three main categories: (i) dark-to-bright photoactivators that convert from a dark state into a bright fluorescent state (also called photoactivatable fluorescent proteins); (ii) reversible highlighters that enable on/off photoswitching at their spectrum (also called photoswitchable fluorescent proteins); (iii) irreversible photoconverters that change their excitation emission spectra (also known as photoconvertible fluorescent proteins) [20,21].

(1) Photoactivatable fluorescent proteins (PA-FPs). PA-FPs possess an initial dark emission state that can be converted into a bright emission state upon UV or violet light exposure. PAGFP, a T203H variant of *Aequorea Victoria* GFP and also the first engineered optical highlighter, initiates a dim green fluorescence when excited at 488 nm and increases fluorescence 100 times after intense irradiation at ~400 nm [22]. When used for SMLM imaging, PAGFP exhibits very high background signals with a low photon burst, together limiting its potential application. It is to note, however, that PAGFP is the only pure green color PA-FP reported to date. For emission in the red part of the spectrum, there are two well-known PA-FPs, namely PAmCherry1 and PATagRFP, both of which exhibit high photoactivation contrast and beneficial single molecule properties [23,24]. PAmCherry1 with maximum excitation/emission at 564/595 nm is derived from mCherry by site-directed screening. Another choice, PATagRFP, mutated from TagRFP, has a 3-fold greater brightness than PAmCherry1 and 540-fold contrast is reported as an excellent fluorescent protein for sptPALM [24].

(2) Photoswitchable fluorescent proteins (PS-FPs). PS-FPs are a big class, and its best-studied member is Dronpa, a non-numeric variant derived from 22G with a maximum excitation/emission at 503/518 nm [25]. A strong 490 nm laser causes bleaching of its fluorescence which turns it into a PAGFP-like dark state, and the bleached protein returns to a bright state with a slight 405 nm laser illumination. The bright state emission of Dronpa is 2.5-fold higher than that of EGFP, however, its single molecule property is not very good given its low total photon number. Our lab developed a series of novel PS-FPs, monomeric Green EosFP (named mGeos), all derived from the EosFP family [26]. One of its members, mGeos-M, exhibits the highest photon budget and localization precision among all PS-FPs, which makes it a suitable partner of PAmCherry1 for dual-color SMLM imaging (Figure 2). The enhanced yellow fluorescent protein (EYFP) with its high localization precision also shown to be an excellent candidate to replace Dronpa for SMLM imaging, and it was first used to image live *Caulobactercrescentus* cells [27]. However, the on/off switching property of EYFP is less than that for Dronpa and members of the mGeos family.

Several other PS-FPs of different colors have been developed for SMLM imaging. A cyan FP, called mTFP0.7, is a by-product of mTFP1, and was reported to be photoswitching on/off multiple times, however, its single molecule property has not been characterized [28]. There exists various photoswitchable red fluorescent proteins such as Kinding FP (KFP1), mApple, rsCherry, rsCherryRev and rsTagRFP [29–32]. In our hands, mApple proved to be an excellent probe, even though it still exhibits a background signal that is too high to be truly suitable for high-quality SMLM imaging.

(3) Photoconvertible fluorescent proteins (PC-FPs). The class of PC-FPs is the most useful probes for SMLM imaging, and is reported to undertake fluorescent conversion from one wavelength to another by specific light inducing. Generally, the mechanism of photoconversion is based on chromophore extension through backbone cleavage [33] or photo-induced oxidation [34,35]. EosFP from the scleractinian coral *Lobophylliahemprichii*, the first PC-FP used in SMLM imaging, emits bright green fluorescence (516 nm) at initial state and can convert to red fluorescence (581 nm) after being illuminated by violet light (405 nm) [5,36]. Its major disadvantage, however, is the fact that the monomeric EosFP (mEosFP) can only successfully maturate below 30°C. To resolve this problem, many new modified variants such as tandem dimer EosFP (tdEosFP), mEos2, mEosFP*thermo*, mEos3.1 and mEos3.2 have been

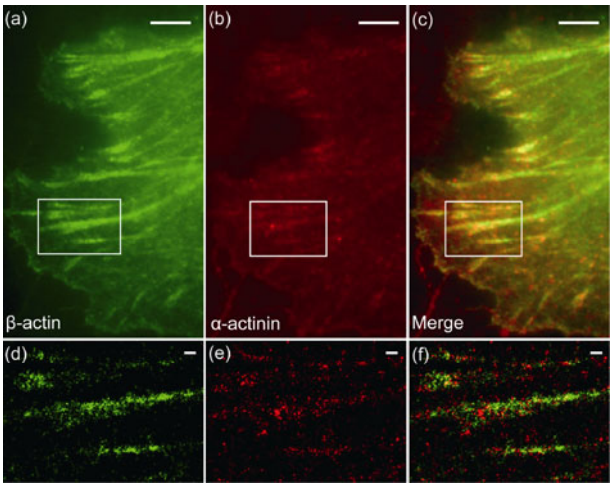

Figure 2 Dual-color PALM imaging. (a) TIRF image of mGeos-M-β-actin. (b) TIRF image of PAmCherry1-α-actinin. (c) Merged dual-color TIRF images, diffraction-limited. (d) PALM image of mGeos-M-β-actin, magnified from the box in (a). (e) PALM image of PAmCherry1-α-actinin, magnified from the box in (b). (f) Merged image of mGeos-M-β-actin (Green) and PAmCherry1-α-actinin (Red). Scale bars are 2 μm in (a)–(c) and 500 nm in (d)–(f). Images reprinted from reference [26].

developed [17,37−39]. The mEos3.2, developed by our group, is a true monomeric protein, which is brighter, faster in maturation and exhibits higher localization precision and labeling density among the PC-FPs [17]. Thus, it can be considered as the most appropriate choice of fluorescent protein for super-resolution imaging. Several other green-to-red fluorescent proteins have been discovered and designed by other laboratories. Kaede was the first reported green-to-red highlighter in 2002, which looks like the initial level of tetramer EosFP [40]. The mechanism of cleavage-based photoconversion as well as some key amino acids required for this type of photoconversion such as His62, Glu212 and Ala69 were obtained by using Kaede as model [33,40]. In an alternative approach, Atsushi Miyawaki's Lab [41] developed a monomeric version of KikGR named mKikGR. Interestingly, mKikGR gives 4500-fold increase in the emission of red color and has been reported to possess very high localization precision. Meanwhile, another groups developed two green-to-red highlighters, namely mClavGR2 and mMaple [42,43]. However, one problem associated with mKikGR, mClavGR2 and mMaple is that all display high pKa values in both the green and red states. Dendra2, the first reported monomeric green-to-red PS-FP, has been widely used in live cell tracking and has proven to be an acceptable probe for single molecule counting with less blinking events [44].

Several additional PC-FPs of different colors have been developed. PS-CFP2 is able to photoconvert from cyan to green under UV light, whereas PSmOrange is capable of photoconversion from orange to far-red, changing both the excitation and emission spectra at the illumination of blue-green light [34,45]. mIrisFP derived from EosFP, and NijiFP derived from Dendra2 with both photoconvertible (green to red) and photoswitchable (both green and red states) properties, shown to be particularly useful in live cell pulse-chase PALM experiments [46,47].

2.2 Synthetic organic fluorophores

The major advantage of synthetic fluorophores and quantum dots is their excellent brightness, outstanding single molecule properties and high labeling density compared to fluorescent proteins. Unfortunately, the experimental conditions required for the use of synthetic fluorophores appear to be more challenging. Investigators need to add STORM buffer containing β-mercaptoethylamine (MEA) or β-mercaptoethanol (βME) with strong laser power or high pH buffer [15,48]. An additional disadvantage is missing target in specific locations, which may lead to the production of artifacts.

Using primary or secondary antibody system is the major choice for SMLM imaging when synthetic fluorophores are employed [7]. However, due to the large size of antibody, a nearly 20 nm localization uncertainty persists, which reduces the localization precision of synthetic fluorophores and quantum dots. The snap-tag, clip-tag or eDHFR-tag is widely used in super-resolution and leads to higher precision in introducing dye-labeled SMLM into live cells [49−51]. A 13-kD antibody (nanobody) with the capability of detecting GFP and single strand DNA or RNA based aptamer combined with dyes are demonstrated as candidates to remove antibody-based systems, hence resolving the encountered size problem [52]. Previously developed dyes (FlAsH, ReAsH, or CHoAsH) are also all found to represent suitable probes for SMLM imaging [53].

3 Developments of single molecule localization microscopy

From the date of its invention, tremendous progress has been made in the use of SMLM in areas like multi-color, three-dimensional (3D) and live cell super-resolution imaging, thus greatly expanding its applicability as well as the scope of use.

3.1 Multi-color imaging

As a general rule, it is not the experimental setup that limits the application of multi-color super-resolution imaging, but the fluorescent probes. The first method achieving two-color super-resolution imaging was PALM with independently running acquisition (PALMIRA) by using β-tubulin labeled with the green PS-FP rsFastLime and Cy5 [54]. Subsequently, two-color STORM experiments were performed using multiple cyanine dye pairings targeting to microtubules and clathrin-coated pits (CCPs) [55]. However, in both cases the fluorescent labels were introduced exogenously, either by conjugation to antibodies or via biotinylation. Soon after, the first two-color PALM experiments were reported using endogenously expressed PA-FP pairs such as Dronpa/EosFP and PS-CFP2/EosFP [56]. This approach offered several advantages but also suffered from the issue of spectral overlap, thus making Dronpa/PS-CFP2 undetectable until all EosFP molecules were imaged and photobleached. A more direct method was then to employ a green marker and a bright red molecule that has no spectral overlap with the green partner, a condition that was made possible with the development of PAmCherry1 and mGoesM [23,26]. As more and more fluorophores are analyzed and evaluated, three or more-color super-resolution imaging experiments have been performed to visualize multiple cellular targets.

3.2 Three-dimensional and whole cell imaging

Early SMLM approaches achieved improvement in resolution in the *x*-*y* direction, not however, in the *z* direction. However, three-dimensional super-resolution imaging is required to truly improve the resolution of complex cellular

structures.

(1) Single objective approaches. 3D STORM was first achieved using a strategy called astigmatism by introducing a weak cylindrical lens (i.e. with a relative long focal length) into the imaging path to create an elliptic spot [57] (Figure 3(a)). The ellipticity and orientation of a fluorophore's image depends on its axial position and hence can be used to compute the z position (Figure 3(a)). Another approach is biplane (BP) imaging which combines PALM with multi-focal imaging to produce a resolution of 30×30×75 nm [58] (Figure 3(b)). The limitation of these two methods is that the maximum depth of field is less or equal than 1 μm. As a result, a third method was implemented using a spatial light modulator to reshape the PSF of emitting light into a double helix pattern. This method, named double-helix PSF (DH-PSF) microscopy, can offer similar resolution in a z range of 2.5 μm [59] (Figure 3(c)).

(2) Opposing objective approaches. Although different approaches had been used to resolve the third dimension, the axial resolution is still lower than the lateral resolution. In order to maximize the number of photons and further enhance the z resolution, opposing objective strategy and interferometry were introduced into conventional super-resolution imaging. The first realization of this scheme, called interferometric PALM (iPALM), has achieved the best resolution with optimal molecular specificity [60]. However, iPALM suffers from the z-dimension ambiguity problem when the imaging layer is thicker than $\lambda/2$ (~225 nm). Therefore, a 4Pi-SMS microscope was constructed to solve the problem by resorting to spherical rather than plane waves [61]. The resolution of 4Pi-SMS microscopy is about the same as iPALM, but the thickness of optical layer can be 1.5λ and placed to any z position in the sample. Besides interferometry, dual-objective schemes can be combined with astigmatism imaging, which further improves the image resolution to less than 20 nm in 3D [62].

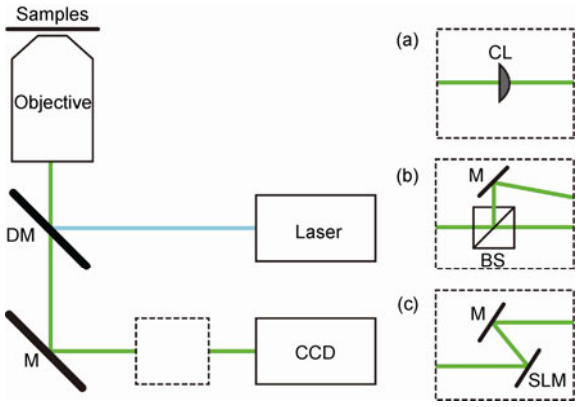

Figure 3 3D super-resolution imaging techniques. The dash box can be configured as different setups such as (a) astigmatism [57], (b) biplane PALM [58] and (c) DH-PSF microscopy [59]. DM: dichroic mirror; M: mirror; CL: cylindrical lens; BS: beam splitter; SLM: spatial light modulator.

(3) Constrained illumination in 3D. In most SMLM approaches, total internal reflection (TIRF) or near TIRF illuminations are employed because of its extremely low background and high signal-to-noise ratio (SNR) [63]. However, the penetration depth of TIRF is restricted to an area close to the surface of the sample (~200 nm), which is not sufficient for whole cell imaging. A simple approach induced with minimal changes to TIRF is called highly inclined and laminated optical (HILO) sheet, which yields clear single-molecule and 3D images when used for cultured mammalian cells [64]. Besides, by using confined activation and two-photon illumination, 3D PALM imaging can be carried out at depths of greater than 8 μm with high localization density [65]. Similarly, through combination of selective plane illumination, a method called individual molecule localization-selective plane illumination microscopy (IML-SPIM) was demonstrated to image single molecules in thick scattering specimens without activating or exciting molecules outside the focal plane [66]. Also, this method was further improved by coupling with two-photon illumination [67]. These illumination techniques, applied together with 3D localization methods, make it possible to perform whole cell super-resolution imaging.

3.3 Fast and live cell imaging

SMLM is confined by a persistent trade-off between spatial and temporal resolution. In fixed cell imaging, the temporal resolution is commonly sacrificed to obtain the best spatial resolution. This is not the case in live cell imaging, when a Nyquist resolution should be considered apart from the localization precision. Therefore, the temporal resolution is limited by the time required to accumulate sufficient numbers of single molecules to produce the desired Nyquist resolution. By using genetically expressed fluorescent proteins, a spatial resolution of ~60 nm in 2D with a time resolution of 30–60 s was achieved [18]. As synthetic dyes always emit much more photons than fluorescent proteins, they can serve as better candidates for live cell imaging. For example, a Nyquist resolution of ~20 nm with a time resolution as high as 0.5 s for 2D STORM imaging was achieved when Alexa Fluor 647 (Alexa 647) was used to label the cells [50]. Besides, anti-GFP nanobodies were employed to encode GFP proteins, which solved the problem arising from the use of full-sized antibodies [52]. Furthermore, 3D super-resolution images of transferrin were acquired with an overall resolution of 30 nm in the x-y dimension and 50 nm in the z dimension at time resolutions as fast as 1–2 s by using photoswitchable cyanine dyes via a SNAP tag in live cells [50]. Remarkably, photoswitchable membrane probes were developed to directly label specific membrane structures and achieve dynamic super-resolution imaging in living cells [68]. In addition, a new method termed sptPALM was created by combining PALM with single particle tracking [13]. This approach offers novel

opportunities to investigate the dynamic behavior of membrane proteins, and provides valuable insights into the origins of spatial and temporal heterogeneities in membranes (Figure 4).

4 Single molecule localization algorithms

The effective spatial resolution of SMLM depends on localization precision and Nyquist resolution. The sub-diffraction limit localization precision lies in the fact that the positions of single molecules can be estimated within several nanometers. Hence, to improve the resolving ability of SMLM, large amount of efforts had been made to develop localization algorithms to approach the fundamental limit.

4.1 Single molecule localization

Due to the shape similarity, a 2D Gaussian function is commonly used to approximate the PSF. Single molecules can be localized either by nonlinear least-squares fitting or maximum-likelihood estimation. The latter was proven to be of higher precision [69]. In addition, this process can be accelerated thousands of times with a graphic processing unit (GPU), thus achieving real-time analysis processing [70]. Also, several other algorithms were developed to speed up the localization without fitting, such as fluoros-Bancroft method [71] and radial symmetry method [72].

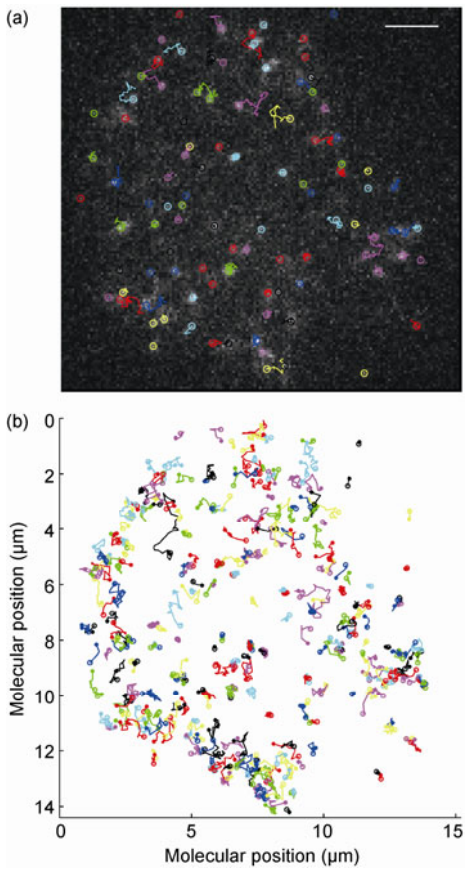

Figure 4 Live cell super-resolution imaging by sptPALM. (a) Single molecule image of Orai1-tdEosFP in HEK293 cells. Scale bar is 2 μm. (b) The trajectories of molecules lasting for more than 1 s are plotted as different colors to distinguish individual tracks.

4.2 Multiple emitters fitting

In order to improve the temporal resolution of SMLM, it is of paramount importance to acquire sufficient numbers of single molecules, thus reaching the Nyquist criterion as quickly as possible. In such situation, the high-density-activated fluorophores will certainly overlap, making it unavailable for performing of single molecule fitting. Several approaches have been reported to address this problem. By simultaneously fitting of overlapping molecules with multiple model PSFs, rather than a single one, DAOSTORM can be applied to high-density imaging analysis up to ~10 molecules/μm^2 [73]. Recently, this method has been extended to 3D super-resolution imaging with astigmatism microscopy. Additionally, an approach using compressed sensing displayed the ability to work with much higher molecule densities compared to DAOSTORM, achieving live cell imaging with a temporal resolution of about 3 s [74]. Another approach which utilizes iterative image deconvolution also enables a fivefold or greater increase in imaging speed by allowing a higher density of activated fluorophores/frame [75]. The common drawback of above methods is that the computational speed is very slow, a problem that was solved by implementing a multiple-emitter fitting algorithm onto a GPU architecture, resulting in analysis times in the order of minutes [76].

4.3 Localization by temporal fluctuations

A different category of localization methods relies on the temporal fluctuations of fluorescence emission. One such strategy of them called super-resolution optical fluctuation imaging (SOFI), relies on higher-order statistical analysis of temporal fluctuations and can be applied to any kind of fluorescence imaging method [77]. Two similar approaches called bleaching/blinking assisted localization microscopy (BaLM) and generalized single molecule high-resolution imaging with photobleaching (gSHRImP), rely on the intrinsic bleaching and blinking behavioral characteristics of fluorophores as a way to overcome the diffraction limit [78,79]. By modeling the entire dataset simultaneously, another method called Bayesian localization microscopy (3B) was able to use each reappearance of a single molecule to improve the localization accuracy and generates a density map of the positions of fluorophores yielded [80]. These methods can be applied to multiple conventional fluorescent probes, and in some cases, do not even require controlled or synchronized photoactivation of lasers.

4.4 Drift correction

Super-resolution images of SMLM are reconstructed from thousands of frames which contain many individual molecules. Hence, this method suffers from sample or instrument drift caused by temperature changes or mechanical instabilities, limiting the spatial resolution. In earlier experiments, fiduciary markers, such as fluorescent beads, gold nanoparticles or quantum dots, were introduced for drift correction due to their strong photostabilities [5,7]. However, the concentration of the markers should be well controlled to obtain satisfactory results. Besides, fiduciary markers made from a polymer were imaged through infrared light illumination and detected using an inexpensive camera [81]. The resulting motion of the coverslip can then be corrected. An alternative method is to utilize the cross-correlation of the images themselves to measure and compensate for any drift, which has proved to be easily implemented and shown to be as an effective method as using fiduciary markers [82,83].

5 Prospects and discussion

SMLM has made huge progress in just a few years and has been applied to every area of biological research. These improvements can be integrated with other methods to create new techniques. Electron microscopy (EM) has been a default imaging method to provide a resolution level well beyond light microscopy. However, with a strategy of fluorophore caging, SMLM has already achieved a resolution of 1–3 nm, which is comparable with EM [84]. Each of the two methods has its specific strengths and weaknesses, but a combination of them, called correlative light electron microscopy (CLEM), has been proved to be a powerful and promising approach to bridge the gap between fluorescence microscopy and EM [85]. For example, PALM has been combined with EM to localize a mitochondrial protein, and iPALM is used with scanning EM, which extends its application to 3D [86,87].

It is not easy for non-experts to keep up with the fast pace of SMLM. Fortunately, major microscopy companies such as Carl Zeiss and Nikon have already provided commercial systems for this type of super-resolution imaging approaches, making SMLM a convenient method accessible to non-expert users. Moreover, several open-source software programs have been developed recently, allowing for simultaneous data acquisition and processing, such as QuickPALM and RapidSTORM, enabling researchers to visualize the reconstruction results in real-time [88,89].

Despite these breakthroughs, SMLM still faces a number of challenges. Compared to STED/SSIM, SMLM has the inherent drawback of requiring special fluorescent probes. For fluorescent proteins, improvements in photon budgets, photoconversion efficiencies and monomer characteristics are still desirable. For synthetic dyes and quantum dots, it is important to develop new labeling methods that can stain the target with small molecule at high specificity, high density and good ultrastructure preservation. For multi- color imaging, the crosstalk between different color channels may produce artifacts and therefore requires correction. In addition, precise alignment should be performed before performing quantitative co-localization analysis. Furthermore, photo-damage caused by intensive illumination and chemical toxicity introduced by imaging buffers (i.e. MEA and βME) should be minimized, especially in live cell imaging. Since the Nyquist criterion specifies that the image sampling interval must be smaller than half of the desired resolution, it is necessary to develop more sensitive detectors/cameras together with fast-switching optical elements to further speed up image acquisition and increase the temporal resolution. Because of optical aberration and distortion, imaging thick issues or structures deep inside cells remains a veritable challenge, and adaptive optics may prove to be the optimal choice [90]. The resolution of an SMLM image largely depends on the precision with which the molecules are localized, so it is susceptible to sample drift. While the 2D drift correction can be easily performed by imaging fiduciary markers such as fluorescent beads, the drift in axial direction always exists and will affect the spatial resolution. Besides, the commonly used Gaussian function is not the true PSF, which will produce systematic errors depending on the dipole orientation and the amount of defocus [91,92]. Although great efforts had been made to reduce this kind of error, it has not been solved yet in a satisfactory manner. Nevertheless, every new technique must overcome its initial teething problems, before developing into powerful new instruments for discovering cellular details thus far unknown to mankind. The innovation and ingenuity of SMLM gives us confidence that super-resolution imaging will become a common tool in the near future.

This work was supported by the National Natural Science Foundation of China (*31130065, 31127002, 31100615 and 31100596*) *and the Chinese Academy of Sciences Project* (*yg2012029*).

1 Hell S W, Wichmann J. Breaking the diffraction resolution limit by stimulated emission: Stimulated-emission-depletion fluorescence microscopy. Opt Lett, 1994, 19: 780–782
2 Hofmann M, Eggeling C, Jakobs S, et al. Breaking the diffraction barrier in fluorescence microscopy at low light intensities by using reversibly photoswitchable proteins. Proc Natl Acad Sci USA, 2005, 102: 17565–17569
3 Gustafsson M G. Surpassing the lateral resolution limit by a factor of two using structured illumination microscopy. J Microsc, 2000, 198: 82–87
4 Gustafsson M G. Nonlinear structured-illumination microscopy: Wide-field fluorescence imaging with theoretically unlimited resolution. Proc Natl Acad Sci USA, 2005, 102: 13081–13086
5 Betzig E, Patterson G H, Sougrat R, et al. Imaging intracellular fluorescent proteins at nanometer resolution. Science, 2006, 313: 1642–1645
6 Hess S T, Girirajan T P, Mason M D. Ultra-high resolution imaging by fluorescence photoactivation localization microscopy. Biophys J, 2006, 91: 4258–4272
7 Rust M J, Bates M, Zhuang X. Sub-diffraction-limit imaging by stochastic optical reconstruction microscopy (storm). Nat Methods,

2006, 3: 793–795
8 Heilemann M, van de Linde S, Schuttpelz M, et al. Subdiffraction-resolution fluorescence imaging with conventional fluorescent probes. Angew Chem Int Ed, 2008, 47: 6172–6176
9 Thompson R E, Larson D R, Webb W W. Precise nanometer localization analysis for individual fluorescent probes. Biophys J, 2002, 82: 2775–2783
10 Ober R J, Ram S, Ward E S. Localization accuracy in single-molecule microscopy. Biophys J, 2004, 86: 1185–1200
11 Schoen I, Ries J, Klotzsch E, et al. Binding-activated localization microscopy of DNA structures. Nano Lett, 2011, 11: 4008–4011
12 Kiel A, Kovacs J, Mokhir A, et al. Direct monitoring of formation and dissociation of individual metal complexes by single-molecule fluorescence spectroscopy. Angew Chem Int Ed, 2007, 46: 3363–3366
13 Manley S, Gillette J M, Patterson G H, et al. High-density mapping of single-molecule trajectories with photoactivated localization microscopy. Nat Methods, 2008, 5: 155–157
14 Lee S H, Shin J Y, Lee A, et al. Counting single photoactivatable fluorescent molecules by photoactivated localization microscopy (palm). Proc Natl Acad Sci USA, 2012, 109: 17436–17441
15 Dempsey G T, Vaughan J C, Chen K H, et al. Evaluation of fluorophores for optimal performance in localization-based super-resolution imaging. Nat Methods, 2011, 8: 1027–1036
16 Zhu Z J, Yeh Y C, Tang R, et al. Stability of quantum dots in live cells. Nat Chem, 2011, 3: 963–968
17 Zhang M, Chang H, Zhang Y, et al. Rational design of true monomeric and bright photoactivatable fluorescent proteins. Nat Methods, 2012, 9: 727–729
18 Shroff H, Galbraith C G, Galbraith J A, et al. Live-cell photoactivated localization microscopy of nanoscale adhesion dynamics. Nat Methods, 2008, 5: 417–423
19 Lakadamyali M, Babcock H, Bates M, et al. 3D multicolor super-resolution imaging offers improved accuracy in neuron tracing. PLoS One, 2012, 7: e30826
20 Patterson G, Davidson M, Manley S, et al. Superresolution imaging using single-molecule localization. Annu Rev Phys Chem, 2010, 61: 345–367
21 Lippincott-Schwartz J, Patterson G H. Photoactivatable fluorescent proteins for diffraction-limited and super-resolution imaging. Trends Cell Biol, 2009, 19: 555–565
22 Patterson G H, Lippincott-Schwartz J. A photoactivatable gfp for selective photolabeling of proteins and cells. Science, 2002, 297: 1873–1877
23 Subach F V, Patterson G H, Manley S, et al. Photoactivatable mcherry for high-resolution two-color fluorescence microscopy. Nat Methods, 2009, 6: 153–159
24 Subach F V, Patterson G H, Renz M, et al. Bright monomeric photoactivatable red fluorescent protein for two-color super-resolution sptpalm of live cells. J Am Chem Soc, 2010, 132: 6481–6491
25 Ando R, Mizuno H, Miyawaki A. Regulated fast nucleocytoplasmic shuttling observed by reversible protein highlighting. Science, 2004, 306: 1370–1373
26 Chang H, Zhang M, Ji W, et al. A unique series of reversibly switchable fluorescent proteins with beneficial properties for various applications. Proc Natl Acad Sci USA, 2012, 109: 4455–4460
27 Biteen J S, Thompson M A, Tselentis N K, et al. Super-resolution imaging in live caulobacter crescentus cells using photoswitchable eyfp. Nat Methods, 2008, 5: 947–949
28 Henderson J N, Ai H W, Campbell R E, et al. Structural basis for reversible photobleaching of a green fluorescent protein homologue. Proc Natl Acad Sci USA, 2007, 104: 6672–6677
29 Chudakov D M, Belousov V V, Zaraisky A G, et al. Kindling fluorescent proteins for precise *in vivo* photolabeling. Nat Biotechnol, 2003, 21: 191–194
30 Shaner N C, Lin M Z, McKeown M R, et al. Improving the photostability of bright monomeric orange and red fluorescent proteins. Nat Methods, 2008, 5: 545–551
31 Stiel A C, Andresen M, Bock H, et al. Generation of monomeric reversibly switchable red fluorescent proteins for far-field fluorescence nanoscopy. Biophys J, 2008, 95: 2989–2997
32 Subach F V, Zhang L, Gadella T W, et al. Red fluorescent protein with reversibly photoswitchable absorbance for photochromic fret. Chem Biol, 2010, 17: 745–755
33 Mizuno H, Mal T K, Tong K I, et al. Photo-induced peptide cleavage in the green-to-red conversion of a fluorescent protein. Mol Cell, 2003, 12: 1051–1058
34 Subach O M, Patterson G H, Ting L M, et al. A photoswitchable orange-to-far-red fluorescent protein, psmorange. Nat Methods, 2011, 8: 771–777
35 Bogdanov A M, Mishin A S, Yampolsky I V, et al. Green fluorescent proteins are light-induced electron donors. Nat Chem Biol, 2009, 5: 459–461
36 Wiedenmann J, Ivanchenko S, Oswald F, et al. Eosfp, a fluorescent marker protein with UV-inducible green-to-red fluorescence conversion. Proc Natl Acad Sci USA, 2004, 101: 15905–15910
37 McKinney S A, Murphy C S, Hazelwood K L, et al. A bright and photostable photoconvertible fluorescent protein. Nat Methods, 2009, 6: 131–133
38 Nienhaus G U, Nienhaus K, Holzle A, et al. Photoconvertible fluorescent protein eosfp: Biophysical properties and cell biology applications. Photochem Photobiol, 2006, 82: 351–358
39 Wiedenmann J, Gayda S, Adam V, et al. From eosfp to mirisfp: Structure-based development of advanced photoactivatable marker proteins of the gfp-family. J Biophotonics, 2011, 4: 377–390
40 Ando R, Hama H, Yamamoto-Hino M, et al. An optical marker based on the UV-induced green-to-red photoconversion of a fluorescent protein. Proc Natl Acad Sci USA, 2002, 99: 12651–12656
41 Habuchi S, Tsutsui H, Kochaniak A B, et al. Mkikgr, a monomeric photoswitchable fluorescent protein. PLoS One, 2008, 3: e3944
42 Hoi H, Shaner N C, Davidson M W, et al. A monomeric photoconvertible fluorescent protein for imaging of dynamic protein localization. J Mol Biol, 2010, 401: 776–791
43 McEvoy A L, Hoi H, Bates M, et al. Mmaple: A photoconvertible fluorescent protein for use in multiple imaging modalities. PLoS One, 2012, 7: e51314
44 Gurskaya N G, Verkhusha V V, Shcheglov A S, et al. Engineering of a monomeric green-to-red photoactivatable fluorescent protein induced by blue light. Nat Biotechnol, 2006, 24: 461–465
45 Chudakov D M, Verkhusha V V, Staroverov D B, et al. Photoswitchable cyan fluorescent protein for protein tracking. Nat Biotechnol, 2004, 22: 1435–1439
46 Fuchs J, Bohme S, Oswald F, et al. A photoactivatable marker protein for pulse-chase imaging with superresolution. Nat Methods, 2010, 7: 627–630
47 Adam V, Moeyaert B, David C C, et al. Rational design of photoconvertible and biphotochromic fluorescent proteins for advanced microscopy applications. Chem Biol, 2011, 18: 1241–1251
48 van de Linde S, Loschberger A, Klein T, et al. Direct stochastic optical reconstruction microscopy with standard fluorescent probes. Nat Protoc, 2011, 6: 991–1009
49 Wombacher R, Heidbreder M, van de Linde S, et al. Live-cell super-resolution imaging with trimethoprim conjugates. Nat Methods, 2010, 7: 717–719
50 Jones S A, Shim S H, He J, et al. Fast, three-dimensional super-resolution imaging of live cells. Nat Methods, 2011, 8: 499–508
51 Klein T, Loschberger A, Proppert S, et al. Live-cell dstorm with snap-tag fusion proteins. Nat Methods, 2011, 8: 7–9
52 Ries J, Kaplan C, Platonova E, et al. A simple, versatile method for gfp-based super-resolution microscopy via nanobodies. Nat Methods, 2012, 9: 582–584
53 Lelek M, Di Nunzio F, Henriques R, et al. Superresolution imaging of hiv in infected cells with flash-palm. Proc Natl Acad Sci USA, 2012, 109: 8564–8569
54 Bock H, Geisler C, Wurm C A, et al. Two-color far-field fluorescence nanoscopy based on photoswitchable emitters. Appl Phys B, 2007, 88: 161–165
55 Bates M, Huang B, Dempsey G T, et al. Multicolor super-resolution imaging with photo-switchable fluorescent probes. Science, 2007, 317: 1749–1753
56 Shroff H, Galbraith C G, Galbraith J A, et al. Dual-color superresolution imaging of genetically expressed probes within individual adhesion complexes. Proc Natl Acad Sci USA, 2007, 104:

20308–20313
57 Huang B, Wang W Q, Bates M, et al. Three-dimensional super-resolution imaging by stochastic optical reconstruction microscopy. Science, 2008, 319: 810–813
58 Juette M F, Gould T J, Lessard M D, et al. Three-dimensional sub-100 nm resolution fluorescence microscopy of thick samples. Nat Methods, 2008, 5: 527–529
59 Pavani S R, Thompson M A, Biteen J S, et al. Three-dimensional, single-molecule fluorescence imaging beyond the diffraction limit by using a double-helix point spread function. Proc Natl Acad Sci USA, 2009, 106: 2995–2999
60 Shtengel G, Galbraith J A, Galbraith C G, et al. Interferometric fluorescent super-resolution microscopy resolves 3D cellular ultrastructure. Proc Natl Acad Sci USA, 2009, 106: 3125–3130
61 Baddeley D, Crossman D, Rossberger S, et al. 4D super-resolution microscopy with conventional fluorophores and single wavelength excitation in optically thick cells and tissues. PLoS One, 2011, 6: e20645
62 Xu K, Babcock H P, Zhuang X. Dual-objective storm reveals three-dimensional filament organization in the actin cytoskeleton. Nat Methods, 2012, 9: 185–188
63 Axelrod D, Burghardt T P, Thompson N L. Total internal reflection fluorescence. Annu Rev Biophys Bioeng, 1984, 13: 247–268
64 Tokunaga M, Imamoto N, Sakata-Sogawa K. Highly inclined thin illumination enables clear single-molecule imaging in cells. Nat Methods, 2008, 5: 159–161
65 York A G, Ghitani A, Vaziri A, et al. Confined activation and subdiffractive localization enables whole-cell palm with genetically expressed probes. Nat Methods, 2011, 8: 327–333
66 Cella Z F, Lavagnino Z, Perrone D M, et al. Live-cell 3D super-resolution imaging in thick biological samples. Nat Methods, 2011, 8: 1047–1049
67 Truong T V, Supatto W, Koos D S, et al. Deep and fast live imaging with two-photon scanned light-sheet microscopy. Nat Methods, 2011, 8: 757–760
68 Shim S H, Xia C, Zhong G, et al. Super-resolution fluorescence imaging of organelles in live cells with photoswitchable membrane probes. Proc Natl Acad Sci USA, 2012, 109: 13978–13983
69 Abraham A V, Ram S, Chao J, et al. Quantitative study of single molecule location estimation techniques. Opt Express, 2009, 17: 23352–23373
70 Smith C S, Joseph N, Rieger B, et al. Fast, single-molecule localization that achieves theoretically minimum uncertainty. Nat Methods, 2010, 7: 373–375
71 Hedde P N, Fuchs J, Oswald F, et al. Online image analysis software for photoactivation localization microscopy. Nat Methods, 2009, 6: 689–690
72 Parthasarathy R. Rapid, accurate particle tracking by calculation of radial symmetry centers. Nat Methods, 2012, 9: 724–726
73 Holden S J, Uphoff S, Kapanidis A N. Daostorm: An algorithm for high-density super-resolution microscopy. Nat Methods, 2011, 8: 279–280
74 Zhu L, Zhang W, Elnatan D, et al. Faster storm using compressed sensing. Nat Methods, 2012, 9: 721–723
75 Mukamel E A, Babcock H, Zhuang X W. Statistical deconvolution for superresolution fluorescence microscopy. Biophys J, 2012, 102: 2391–2400
76 Huang F, Schwartz S L, Byars J M, et al. Simultaneous multiple-emitter fitting for single molecule super-resolution imaging. Biomedical Optics Express, 2011, 2: 1377–1393
77 Dertinger T, Colyer R, Iyer G, et al. Fast, background-free, 3D super-resolution optical fluctuation imaging (sofi). Proc Natl Acad Sci USA, 2009, 106: 22287–22292
78 Burnette D T, Sengupta P, Dai Y, et al. Bleaching/blinking assisted localization microscopy for superresolution imaging using standard fluorescent molecules. Proc Natl Acad Sci USA, 2011, 108: 21081–21086
79 Simonson P D, Rothenberg E, Selvin P R. Single-molecule-based super-resolution images in the presence of multiple fluorophores. Nano Lett, 2011, 11: 5090–5096
80 Cox S, Rosten E, Monypenny J, et al. Bayesian localization microscopy reveals nanoscale podosome dynamics. Nat Methods, 2012, 9: 195–200
81 Lee S H, Baday M, Tjioe M, et al. Using fixed fiduciary markers for stage drift correction. Opt Express, 2012, 20: 12177–12183
82 Geisler C, Hotz T, Schonle A, et al. Drift estimation for single marker switching based imaging schemes. Opt Express, 2012, 20: 7274–7289
83 Mlodzianoski M J, Schreiner J M, Callahan S P, et al. Sample drift correction in 3D fluorescence photoactivation localization microscopy. Opt Express, 2011, 19: 15009–15019
84 Vaughan J C, Jia S, Zhuang X. Ultrabright photoactivatable fluorophores created by reductive caging. Nat Methods, 2012, 9: 1181–1184
85 van Rijnsoever C, Oorschot V, Klumperman J. Correlative light-electron microscopy (CLEM) combining live-cell imaging and immunolabeling of ultrathin cryosections. Nat Methods, 2008, 5: 973–980
86 Watanabe S, Punge A, Hollopeter G, et al. Protein localization in electron micrographs using fluorescence nanoscopy. Nat Methods, 2011, 8: 80–84
87 Kopek B G, Shtengel G, Xu C S, et al. Correlative 3D super-resolution fluorescence and electron microscopy reveal the relationship of mitochondrial nucleoids to membranes. Proc Natl Acad Sci USA, 2012, 109: 6136–6141
88 Henriques R, Lelek M, Fornasiero E F, et al. Quickpalm: 3D real-time photoactivation nanoscopy image processing in image. Nat Methods, 2010, 7: 339–340
89 Wolter S, Loschberger A, Holm T, et al. Rapidstorm: Accurate, fast open-source software for localization microscopy. Nat Methods, 2012, 9: 1040–1041
90 Ji N, Milkie D E, Betzig E. Adaptive optics via pupil segmentation for high-resolution imaging in biological tissues. Nat Methods, 2010, 7: 141–147
91 Stallinga S, Rieger B. Accuracy of the gaussian point spread function model in 2D localization microscopy. Opt Express, 2010, 18: 24461–24476
92 Engelhardt J, Keller J, Hoyer P, et al. Molecular orientation affects localization accuracy in superresolution far-field fluorescence microscopy. Nano Lett, 2011, 11: 209–213

Supporting Information

Table S1 Properties of selected optical highlighter fluorescent protein derivatives

The supporting information is available online at csb.scichina.com and www.springerlink.com. The supporting materials are published as submitted, without typesetting or editing. The responsibility for scientific accuracy and content remains entirely with the authors.